# Nonelectric, Standalone Heating Element for an Infant Incubator

by

Stephanie A. Whalen

Submitted to the Department of Mechanical Engineering
in Partial Fulfillment of the Requirements for the Degree of

Bachelor of Science in Mechanical Engineering

at the

MASSACHUSETTS INSTITUTE OF TECHNOLOGY

June 2012



Signature of Author . . . . . .
Department of Mechanical Engineering
May 17, 2012

Certified by . . . . . .
Sanjay E. Sarma
Professor of Mechanical Engineering
Thesis Supervisor

Accepted by . . . . . .
John H. Lienhard V
Samuel C. Collins Professor of Mechanical Engineering
Undergraduate Officer

**Nonelectric, Standalone Heating Element for an Infant Incubator**

by

Stephanie A. Whalen

Submitted to the Department of Mechanical Engineering
on May 17, 2012 in Partial Fulfillment of the
Requirements for the Degree of

Bachelor of Science in Mechanical Engineering

## Abstract

Anya is an incubator design intended for use in the developing world. It aims to reduce the instances of premature infant death in the developing world, specifically targeting places where household electricity is uncommon. Thus, Anya requires a nonelectric heating method. Paraffin wax, a phase change material with high latent heat storage, was selected as the heating element for study. The wax can be melted in boiling water, used to deliver heat to the incubator, then melted again once the material has solidified.

A one-dimensional thermal circuit model was developed to predict the thermal behaviors of the incubator as a function of the thermal resistances of the materials used and ambient air temperature. The thermal behaviors studied were steady-state temperature, duration of heating element usage, and time for the air chamber to reach steady-state temperature.

By melting quantities of wax, placing it in coolers with plastic container lids, and measuring the temperature response over time, the mathematical model was evaluated. The tests were difficult to compare to the model, as nonuniform melting temperatures of the wax and lack of airtight containers for the tests caused irregularities in the results. However, the simulations' behavior implicated two features the model should incorporate for future study: (1) the thermal resistance and temperature gradients within the air chamber, and (2) the thermal capacitance of the resistive materials used between the wax and the air chamber.

Thesis Supervisor: Sanjay Sarma
Title: Professor of Mechanical Engineering

# Acknowledgments

I would like to acknowledge Stephen Ho for his innumerable contributions to my model, as well as Sanjay Sarma for advising this project. I would like to thank Subhrangshu Datta and Chitro Neogy for their continuous support of the Anya work being done at MIT.

I would like to thank my parents for their patience and cooperation in using their kitchen and living room for one of my experiments. Special thanks go to my mother, Kim, and my grandmother, Nancy, for their countless hours of editing sections of my thesis for clarity and grammar that no one else has the patience for correcting.

I would like to thank my grandfather, Dennis, for his edits as well, which helped strengthen the arguments made in the thesis and address limitations of the research. After finishing drafts at four in the morning, I could count on my grandfather to return them with his insightful comments in the PDF six hours later, even before I had woken up.

I would like to thank Claire Kearns-McCoy and Mary Breton for providing their feedback on my thesis, even when they were busy with their own coursework.

I would like to wholeheartedly thank my entire family, friends, and sorority for their unwavering support throughout my years at MIT. Special thanks to Jessica Hammond for her support and teamwork in completing our theses.

# Contents

# List of Figures

# List of Tables

# Introduction

The market for medical devices in India is growing (see Figure 0.1). Products that will best penetrate this market will be of high quality, but affordable. In general, competitive products for the developing world market must be durable and low-maintenance. Great products for this market provide independence from electricity and are easily serviceable by local professionals or through the mail.

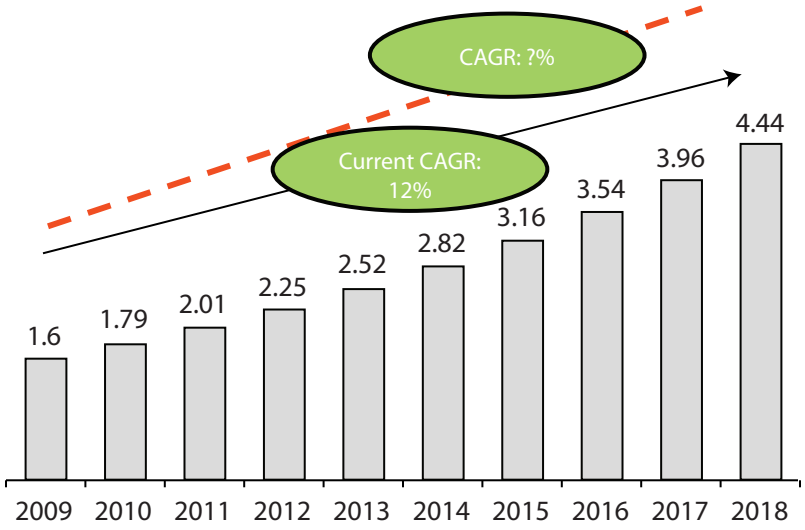


**Figure 0.1:** Projected medical device market in India, in billions of USD. The current compound annual growth rate (CAGR) is an attractive 12%. Source: Pacific Bridge Medical. Figure graphic from Datta and Neogy [1].

Approximately 7,400 premature infants die every day in the developing world. Of those deaths, 5,900 of them occur in the home, where people have no access to incubators. In 2011, 9 million of the 12 million premature births in the developing world occurred in homes. Premature infant mortality is only slightly lower in smaller hospitals, the site of 1,500 premature infant deaths per day. In smaller hospitals in the developing world, incubation systems are not readily available, medical professionals often have limited training, and cross-contamination is common [1].

## Incubation Solutions Available Today

Currently available mobile incubators are quite expensive (over $2000 per unit), and impractical for developing countries [1]. GE Healthcare's Airborne 750i Infant Transport Incubator is designed for intra-hospital transport only, and would be too cumbersome to remove from a neonatal intensive care unit (NICU). The Air Shields C300 is also too heavy for transport, and has reliability issues (Figure 0.2) [1].

**Figure 0.2:** Left, GE Airborne 750i Infant Transport Incubator; right, Air Shields C300 (Images from GE Healthcare [2], Whittemore Enterprises [3] respectively).

Besides these options, there are few alternatives. The kangaroo care method, where the mother holds the baby close to her chest or in her clothes, costs nothing, but skin-to-skin contact increases likelihood of infection transfer to the vulnerable premature infant [1].

A Garam bag, an insulation device similar in design to a sleeping bag, is portable, can be used at home, and costs only $1.25 [1]. However, this product is only practical for infants born after proper gestation. Premature infants do not generate heat, and therefore the insulation does little good. This product also has a similar disadvantage to kangaroo care: it does not provide protection from infection transmission.

An innovative product on the market is the Embrace infant warmer (Figure 0.3). It is also shaped like a sleeping bag, but incorporates a phase change material (PCM) that steadily releases heat.

Heating the Embrace's WarmPak requires the exclusive use of the AccuTemp heater (provided with the product), which uses an AC power source (see Figure 0.4). The phase change material provides up to 6 hours of heat [4].

The Embrace sells for $150, more than ten times the expense of the Garam bag, due to the addition of the PCM and heater. The intended users of this product are nurses and doctors, but it is not the elegant solution that many hospitals would hope for, thus unlikely to replace traditional incubators. The cost of $150 is also high for a less comprehensive product designed for developing countries [5]. It also does not provide complete protection from disease transmission, as the infant's face is still exposed.

**Figure 0.3:** The Embrace product includes a sleeping bag-shaped device, the WarmPak (a PCM-filled heating pad, placed in a pouch in the Embrace), and the AccuTemp heater (see Figure 0.4). Image from Embrace [4].

**Figure 0.4:** Heating the Embrace. Image from Embrace [4].

## Anya

This paper focuses on Anya: an innovative, portable incubator design that can be used in both the home and the NICU. Anya was envisioned by Subhrangshu Datta and Chitro Neogy, MIT Sloan graduates and founders of FrontierMed Technologies. FrontierMed Technologies sponsored the work done in this thesis, as well as work by Elaina Present and Delian Asparouhov.

An Anya prototype can be seen in Figure 0.5, and concept sketches of this product can be seen in Figure 0.6. The undergraduate thesis work done by Elaina Present covers the design and manufacturing of this product, and Delian Asparouhov, an undergraduate research student, is currently designing the monitoring system and mobile application [6].

Compared to hospital incubators, Anya will be much less costly and cumbersome, so it can be used in the home. It can be configured for use in both the hospital and the home, will be of a modest size (one child per incubator), and can be carried from a hospital with ease.

Compared to the products resembling sleeping bags (the Garam bag, the Embrace), Anya will provide a heat source and a complete cover for the child for complete protection. Its exterior and docking station will look professional and fit naturally into a NICU setting.

Unlike the Embrace, the goal of Anya is independence from an electric power source, allowing users without electricity in their homes to use the product, and allowing all users with premature infants more mobility in living and traveling. Thus, the focus of this work is to investigate methods for the incubator to provide heat without electricity. Outside of the NICU, a reusable heating element will be used to heat the chamber. The heating element must be boiled and reinserted when

**Figure 0.5:** A 30-week old infant in an Anya prototype at Gangaram Hospital, New Delhi, India. The incubator will also incorporate a cover or shield, not shown. Image from Datta and Neogy [1].

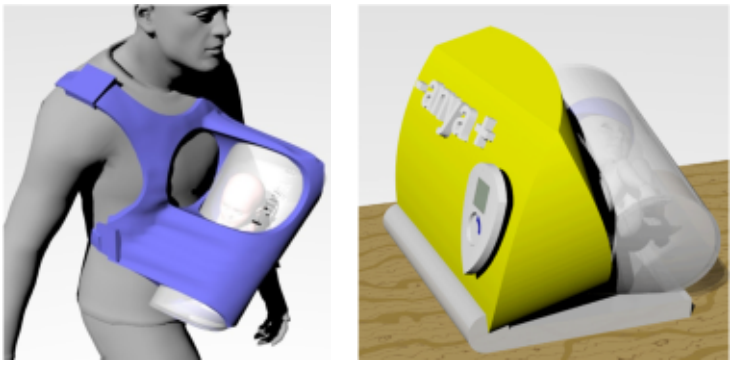


**Figure 0.6:** Anya will be able to transform from a portable, carriable incubator into a hospital-style, stationary incubator with a small footprint. Images from Datta and Neogy [1].

the liquid material has solidified (see Figure 0.7). Boiled water is readily available to families living and traveling in rural parts of the developing world. It is common to find large pots of boiling water along the road for use in making tea, so these can be utilized in reheating the heating element allowing the incubator to be "refueled" in villages near users' homes, and in the hours-long journey to and from the hospital. These pots of water are much more common than electricity, so Anya will be more convenient than the Embrace for both living in areas without electricity and transport.

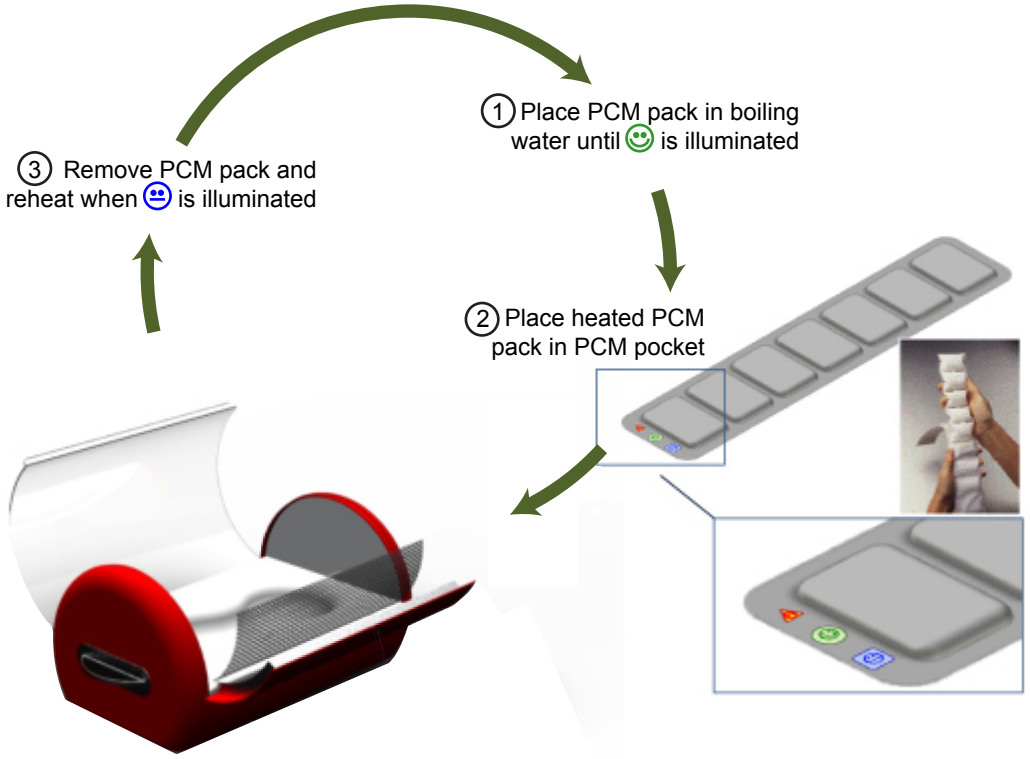


**Figure 0.7:** The envisioned heating method for Anya. Original graphics from Datta and Neogy [1].

## Phase Change Materials

Several phase change materials were investigated for use in the heating pack. A phase change material utilizes latent heat rather than sensible heat to store energy. Energy storage by means of sensible heat is demonstrated by a proportional temperature change. Latent heat is stored in a

material as it changes phase (e.g., from a solid to a liquid), and does not cause temperature change. At low temperatures (around room temperature or just above), materials such as water (which boils at 100°C) simply increases in temperature with the addition of heat. Phase change materials change phases at lower temperatures, so with the addition of heat, they will store the energy in the form of a temperature change until the phase change temperature is reached, then store the amount of latent heat energy required for the phase change until the phase change is complete, then resume absorbing sensible heat energy [7]. One kilogram of water heated from 20°C to 85°C stores about 272 kJ of energy, while one kilogram of paraffin wax heated from 20°C to only 55°C stores about 277 kJ. While water has a much higher heat capacity than paraffin wax (4.184 kJ/kg versus about 2.5 kJ/kg), the latent heat of fusion that paraffin wax can absorb in its phase change is about 200 kJ/kg. Water does not undergo a phase change in the range of incubation temperatures, so it will not store any energy in the form of latent heat.

In selecting a phase change material for study, PCMs were evaluated for cost and latent heat of fusion. Sodium acetate trihydrate initially looked promising. It seemed easy to produce at a low-cost, melts at 58°C, and has a latent heat of fusion of 264-289 kJ/kg [8]. In addition, it is able to remain stable in the liquid state under certain conditions (supercooling), so after melting the used solid in boiling water, it can be stored in liquid form and activated when needed. Agitation (nucleation) of the material causes its solidification (crystallization), initiating its release of heat. However, in initial experimentation, sodium acetate proved difficult to keep in a stable state and tended to self-nucleate, perhaps due to the impurities of laboratory experiments. Thus, there was no distinct advantage to using sodium acetate over a typical, self-nucleating PCM. Paraffin wax, a PCM without a nucleation requirement, was selected for study in this paper, as it has a melting temperature between 58 and 62°C and is a common, inexpensive material [9]. However, most of the theory used in the paper can be applied to any similar material used.

## Anya's Technical Requirements

The technical requirements for this product that need to be considered by the thermal studies in this paper are total weight (under five kilograms, preferably less), a chamber temperature of 31 to 34°C, and provision of heat for two to four hours [1]. This work encompasses modeling of the

heat transfer processes for the incubator, as well as experimentation testing the accuracy of these models.

## Limitations of This Study

The anticipated limitations of the work done in this thesis are the following:

### Thermal Resistance Selection for External Shield

It should be noted that a substantial limitation in this analysis is the restricted number of materials acceptable for use as the outer shield. Parents or caretakers absolutely must be able to visually monitor the child, so the shield must be clear, and not so thick that clarity becomes an issue. Clear acrylic or plexiglass are the most obvious choices. Glass materials are clear, but could be dangerous to the infant if the shield shattered due to an impact. Glass is also very dense and would thus increase weight. Plastic has a relatively low resistance (or, rather, a high thermal conductivity) compared to cotton batting or padding that will cushion the child. Difficulties in obtaining correct ratios of resistances will result from the rigidity of this requirement, and this will affect many future design decisions when using the analysis in this thesis.

### Heat Losses Through the Incubator Body

In this paper, it is assumed that all heat transfers to the outside of the incubator occur through the external shield of the incubator, and not through the body of the incubator. In the final design, a comparison of the thermal resistances of the incubator body and shield will need to be made. For this model to accurately predict the incubator's thermal behaviors, the majority of the heat losses should be through the shield. If this is not the case, the model will need to be adjusted.

### Ventilation Considerations

This paper does not cover ventilation, air exchange, or air circulation devices, which will likely need to be incorporated into the final incubator to provide fresh, clean air to the infant. Any

exchanges of internal and external air will likely cause losses in heat or power, and these losses are not considered in the following sections. The ventilation system will have to be examined, and the models used in this paper will have to be adjusted to reflect the heat and air exchange.

# One-Dimensional Heat Transfer Model

**Undergraduate Thesis Essay 1**

Stephanie A. Whalen

MIT Department of Mechanical Engineering

Cambridge, MA

May 17, 2012

# One-Dimensional Heat Transfer Model


## Abstract

This essay analyzes the idealized one-dimensional heat transfer through the incubator chamber. The incubator is modeled as a simple thermal circuit consisting of a resistor (the material between the air chamber and wax), a capacitor (the air contained in the chamber), and a resistor (the shield between the chamber and the environment) in series.

It is found that the steady-state temperature of the chamber air depends upon the ratio of the resistances chosen for the resistors (like a voltage divider), the external temperature, and the heater temperature. The required heating element mass depends upon the resistances chosen, and exponentially decays in response to an increase in resistances. Two high resistances (above 0.75 K/W) provide an adequate duration of heat for less than one kilogram of wax. The transient response of the air temperature is in the form of a linear first order equation, and the model predicts that the air will take less than three minutes to complete 98% of its rise in temperature. A low resistance provides a faster response time, but at the expense of additional heat source mass required for giving sufficient heating time—a poor trade-off.

The steady-state temperature is found to be quite sensitive to the environmental temperature, even for high resistances. This property should be examined with experiments using various resistances and possibly incubator materials that can be changed for use in various climates. The mass of wax should be selected for the lower environmental temperatures to ensure sufficient usage time. The model predicts no change in response time of the temperature rise in the air chamber for changing external temperatures. This is likely one of the model's several limitations.

## 1.1 Thermal Circuit

The Fourier Law of Conduction, Equation 1.1, states that the rate of heat transfer through a material is proportional to the temperature gradient and the cross-sectional area through which the heat transfer is taking place, viz.

$$\dot{Q} = -kA\frac{dT}{dx} \tag{1.1}$$

where $\frac{dT}{dx}$ is the temperature gradient through the medium, $k$ is the thermal conductivity, and $A$ is the cross-sectional area [10, (6.1)]. For a conduction path of constant cross-sectional area with length, $l$, Equation 1.1 can be integrated from $x = 0$ (where $T = T_a$) to $x = l$ where ($T = T_b$) [10, (6.2)],

$$\dot{Q}\int_0^l dx = -kA\int_{T_a}^{T_b} dT \tag{1.2}$$

or

$$\dot{Q} = \frac{kA}{l}(T_a - T_b). \tag{1.3}$$

More simply, we can let $T_a - T_b = \Delta T$:

$$\dot{Q} = \frac{kA}{l}\Delta T. \tag{1.4}$$

Equation 1.4 can be directly compared to Ohm's law, which states that the current through a resistor is proportional to the voltage drop across the resistor divided by the resistance (Equation 1.5). $\Delta T$ is the "temperature drop" across our thermal resistor.

$$i = \frac{\Delta V}{R} \tag{1.5}$$

Considering these heat transfer equations in terms of thermal resistance allows us to make direct analogies to electrical circuits, which have been extensively studied and thus their behavior is well-known. Thermal resistance is analogous to electrical resistance; as the rate of heat transfer, $\dot{Q}$, is analogous to current, $i$; and temperature drop, $\Delta T$, is analogous to voltage drop, $\Delta V$.

The system boundaries and heat transfers have been defined in Figure 1.1. The values for $\dot{Q}_1$ and

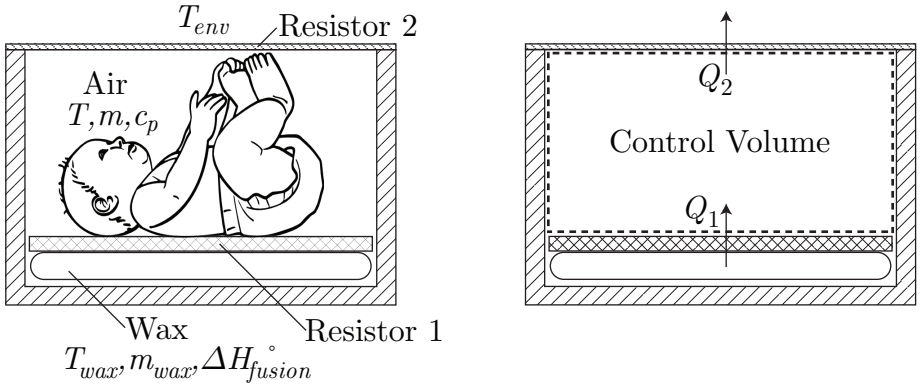


**Figure 1.1:** Left, the incubator with system temperatures and properties. Right, the system boundaries (dashed border) and heat transfers ($Q_1$, $Q_2$) are defined. Baby graphic from [11].

$\dot{Q}_2$ are defined in Equation 1.6 and Equation 1.7, respectively.

$$\dot{Q}_1 = \frac{k_1 A}{l_1}(T_{wax} - T) = \frac{T_{wax} - T}{R_1} \tag{1.6}$$

$$\dot{Q}_2 = \frac{k_2 A}{l_2}(T - T_{env}) = \frac{T - T_{env}}{R_2} \tag{1.7}$$

In the above equations, we see that the thermal resistance of a conducting material can be given by the characteristic length divided by the product of the thermal conductivity of the material and the area, or $R_i = \frac{l_i}{k_i A}$. Besides identifying with the electrical analogy, using $R$ instead of the individual components $l$, $k$, and $A$ allows $R$ to include convection components if necessary (for example, convective resistances, $\frac{1}{h_c A}$, could be added in parallel to conductive components) [10, (6.13),(6.14)].

The following sections use these basic equations to model the steady-state temperatures, heater material mass requirements, and transient air temperature response based on thermal resistances of chosen materials, ambient temperature, and heating element temperature. These properties have a significant impact on the incubator's ability to maintain the infant's temperature as well as on the incubator's usability by the parent or caretaker.

It should be noted that a substantial limitation in this analysis is the restricted number of materials acceptable for use as the outer shield. Parents or caretakers absolutely must be able to visually

monitor the child, so the shield must be clear, and not so thick that clarity becomes an issue. Clear acrylic or plexiglass are the most obvious choices. Glass materials are clear, but could be dangerous to the infant if the shield shattered due to an impact. Glass is also very dense and would thus increase weight. Plastic has a relatively low resistance (or, rather, a high thermal conductivity) compared to cotton batting or padding that will cushion the child. Difficulties in obtaining correct ratios of resistances will result from the rigidity of this requirement, and this will affect many future design decisions when using the analysis in this thesis.

In this paper, it is assumed that all heat transfers to the outside of the incubator occur through the external shield of the incubator, and not through the body of the incubator. In the final design, a comparison of the thermal resistances of the incubator body and shield will need to be made. For this model to accurately predict the incubator's thermal behaviors, the majority of the heat losses should be through the shield. If this is not the case, the model will need to be adjusted.

This paper does not cover ventilation, air exchange, or air circulation devices, which will likely need to be incorporated into the final incubator to provide fresh, clean air to the infant. Any exchanges of internal and external air will likely cause losses in heat or power, and these losses are not considered in the following sections. The ventilation system will have to be examined, and the models used in this paper will have to be adjusted to reflect the heat and air exchange.

### 1.1.1 Steady-State Temperature

At steady state, two resistors in series will have an equal current flowing through them. Similarly for the thermal circuit, at steady-state temperature (i.e., when the temperature of the chamber has reached a constant temperature), the heat flux through the system is constant ($\dot{Q}_1 = \dot{Q}_2$). In the electrical analogy, at steady state, capacitors become fully charged and behave like a wire. Likewise, this model assumes that at steady state, the air temperature is constant throughout the chamber, and the dominant heat transfer occurs where the major temperature gradients are: across resistors 1 and 2. Thus, the capacitance can be ignored. See Figure 1.2.

Setting Equation 1.6 and Equation 1.7 equal to each other (since $\dot{Q}_1 = \dot{Q}_2$) enables us to define one resistance with respect to the other by a ratio of the system temperature drops (Equation 1.8).

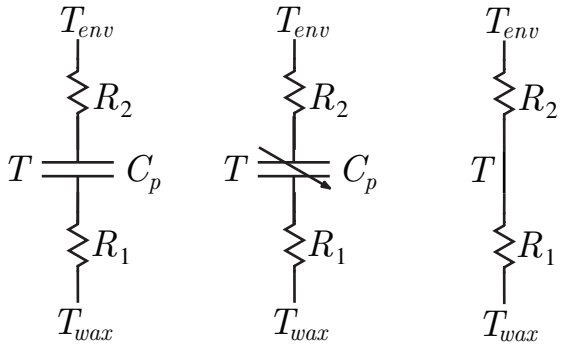


**Figure 1.2:** At steady state, the capacitor is equivalent to a simple electrical wire, and the equivalent circuit is shown on the right. Instead of voltages, temperatures are indicated. Individual circuit elements created in Adobe Illustrator by Swann [12].

Here, $T_f$ is the final (steady-state) temperature.

$$R_2 = R_1 \frac{T_{env} - T_f}{T_f - T_{wax}} \tag{1.8}$$

This property is similar to that of a voltage divider in an electrical circuit, where $R_2 = R_1 \frac{\Delta V_2}{\Delta V_1}$, or $\Delta V_2 = \frac{R_2}{R_2} \Delta V_1$.

The following conclusions can be made from Equation 1.8, assuming environmental and wax temperatures are known:

1. By defining the chamber's steady-state temperature and one resistance, the other resistance can be obtained.

2. Given two resistances, the steady-state temperature can be found.

3. If $T_f$ is 35°C (approximately the desired air temperature for the infant's environment), $T_{wax}$ is 50°C (a low estimate of paraffin melting temperature), and $T_{env}$ is 20°C (i.e. there a 15°C temperature drop from inside to the outside of the chamber and from the heating element to the inside of the chamber), $R_1 = R_2$.

### 1.1.2 Steady State - Calculating the Required Mass

The mass of the incubator can hinder the usability of the product. A large mass of wax not only adds to the weight, but will also be difficult to handle and take a long time to melt during the reheating process. However, a smaller quantity of wax means less energy available for heating the incubator, thus shorter usage times. A balance must be struck between weight and the length of time that the wax provides heat. This section calculates the amount of mass required for the inputs of usage time and resistances. Greater resistances will reduce the heat flux and thus extend the heating time, as high resistances in an electrical circuit reduce the current flowing through the circuit, and therefore extend battery life.

The mass of heating element, $m_{wax}$, required for a certain heating time can be calculated using the substance's latent heat of fusion, $\Delta H^{\circ}_{fusion}$, the material property that defines the change in enthalpy of the substance as it melts. This is an important consideration for choosing the material. Too low of a latent heat of fusion requires that more mass be used, as we will see below. The latent heat of fusion for paraffin wax is between 145 and 240 kJ/kg (paraffin can contain a wide range of hydrocarbons with different properties) ([13], cited by [7]). For modeling purposes, 200 kJ/kg was used.

If we assume that all enthalpy drops occur due to the emission of heat, the overall heat transfer, $Q$, can be found by multiplying the mass of the wax by the latent heat of fusion,

$$Q = m_{wax}\Delta H^{\circ}_{fusion}. \tag{1.9}$$

To solve for the mass required, the overall heat transfer for a heating period must be found. Integrating Equation 1.6 at steady state over the required time period of heating ($t_f$) enables us to find the overall heat transfer, $Q$.

$$Q = \int_0^{t_f} \dot{Q}dt = \int_0^{t_f} \frac{T_{wax} - T_f}{R_1}dt \tag{1.10}$$

Equating Equation 1.9 and Equation 1.10 and solving for mass yields Equation 1.11.

$$m_{wax} = \frac{T_{wax} - T_f}{\Delta H^{\circ}_{fusion}} \frac{t_f}{R_1} \tag{1.11}$$

Figure 1.3 shows the mass of wax required for different lengths of time as resistance increases. Note the differences in mass required between one hour and four hours before and after the point where the slope becomes less than 1 kg/K/W ($R$ =0.75 K/W for the two hour line): the difference is very significant to the left of this point, but much less significant to the right. The difference in required masses at $R = 0.2$ K/W is 4.05 kg (i.e., 4.05 kg more is required for three more hours), whereas at $R = 2$, only 0.405 kg more is need for the three extra hours. Therefore, the resistances selected should be to the right of the change in the magnitude of the slope, as heating time will be more efficient per kilogram of weight added. However, the resistance chosen should not be too far to the right of this change in slope, because insignificant amounts of mass will be saved. It can be seen in the following section that increasing resistance has its costs in other ways, such as a slow system response time.

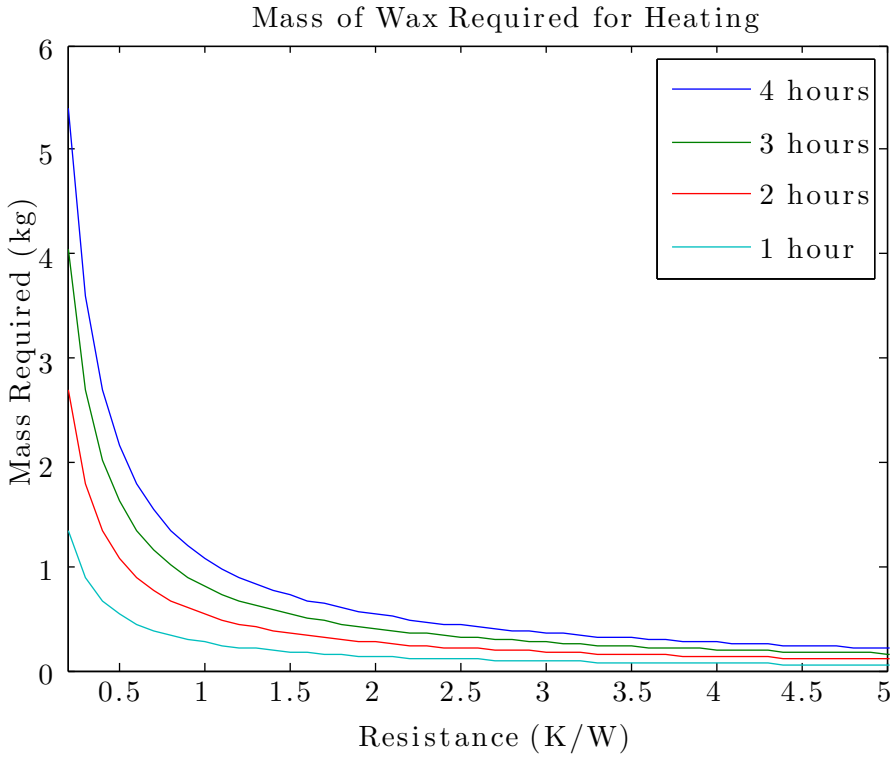


**Figure 1.3:** The graph above shows that the amount of wax required for different lengths of time heat is provided or emitted for a range of resistances, given that the $R_1$ and $R_2$ are equal to one another and the ambient temperature is 20°C.

Based on Figure 1.3, the absolute resistance for parts selected should be greater than 0.75 K/W, as it will be easier to select a sufficiently light mass for a long duration of use.

### 1.1.3 Transient Response

As seen from the previous section, the possible resistances and the ratio between the two resistances must be evaluated for a suitable steady-state temperature. However, the transient response also must be taken into account. This section highlights the effects of chosen resistances on the speed at which the chamber reaches the desired temperature from the starting temperature. It is hypothesized that high resistances between the wax and the chamber will result in a slower transient response. An incubator with a more resistant material or greater thickness of material between the baby and the wax will take a longer time to heat from ambient temperature after the chamber has been closed. This time-dependent model will be compared to experimental data in section 3.2.

#### Derivation of the Ordinary Differential Equation

First, the thermodynamic system being considered is the air-filled chamber, above the first resistive layer which covers the wax, and below the second resistive layer leading to the outside of the chamber, as defined in Figure 1.1. We begin with the first law of thermodynamics in Equation 1.12 [10, (2.9)]:

$$dU = \delta Q - \delta W \tag{1.12}$$

Since no work is being done on the system, the work term is nonexistent.

$$dU = \delta Q - \cancelto{0}{\delta W} \tag{1.13}$$

The internal energy of the system is defined from the energy constitutive relation and written in differential form in Equation 1.14 [10, (3.24)].

$$dU = mc_p dT \tag{1.14}$$

The heat transfer components can be written as a sum of the two heat transfers (across $R_1$ and $R_2$).

$$dQ = dQ_1 + dQ_2 \tag{1.15}$$

From Equation 1.13, Equation 1.14, and Equation 1.15, we get

$$dQ_1 + dQ_2 = mc_p dT. \tag{1.16}$$

Differentiating Equation 1.16 with respect to time, we obtain

$$\dot{Q}_1 + \dot{Q}_2 = mc_p \frac{dT}{dt}. \tag{1.17}$$

$\dot{Q}_1$ and $\dot{Q}_2$ are not explicitly known. However, Equation 1.6 and Equation 1.7 are dependent on $T$, and if the ordinary differential equation is linear, we will be able to solve it. Substituting for $\dot{Q}_1$ and $\dot{Q}_2$ respectively, we see the beginnings of our ODE in Equation 1.18.

$$\frac{T_{wax} - T}{R_1} + \frac{T_{env} - T}{R_2} = mc_p \frac{dT}{dt} \tag{1.18}$$

Rearranging, a final ordinary differential equation of the form $\frac{dx}{dt} + p(x)x = q(x)$ (linear first-order equation) has been discovered [14, Section 1.5, (3)]:

$$\frac{dT}{dt} + \frac{1}{mc_p}\left(\frac{1}{R_1} + \frac{1}{R_2}\right)T = \frac{1}{mc_p}\left(\frac{T_{wax}}{R_1} + \frac{T_{env}}{R_2}\right). \tag{1.19}$$

**Solution of the ODE**

For clarity and simplicity in solving, let

$$F = \frac{1}{mc_p}\left(\frac{1}{R_1} + \frac{1}{R_2}\right) \tag{1.20}$$

and

$$G = \frac{1}{mc_p}\left(\frac{T_{wax}}{R_1} + \frac{T_{env}}{R_2}\right). \tag{1.21}$$

Thus, the ordinary differential equation becomes

$$\frac{dT}{dt} + FT = G. \tag{1.22}$$

The solution to a linear first-order equation like the one above is

$$T(t) = Ce^{-Ft} + \frac{G}{F} \tag{1.23}$$

where C is a constant determined by initial conditions. We know the temperature of the chamber is initially equal to environmental temperature, $T_{env}$ (i.e., $T(t=0) = T_{env}$). From this, it is determined that $C = T_{env} - \frac{G}{F}$. Substituting, we find the solution to the ODE as follows,

$$T(t) = \left(T_{env} - \frac{G}{F}\right) e^{-Ft} + \frac{G}{F}. \tag{1.24}$$

Substituting the values of $F$ and $G$, the final solution to the ODE in terms of physical properties is:

$$T(t) = \left(T_{env} - \frac{(R_1+R_2)(R_1T_{env}+R_2T_{wax})}{R_1^2R_2^2}\right) e^{-\frac{R_1R_2}{mc_p(R_1+R_2)}t} + \frac{(R_1+R_2)(R_1T_{env}+R_2T_{wax})}{R_1^2R_2^2}. \tag{1.25}$$

**Matlab Function**

The function `odetair` was created to simulate the system response after the chamber is opened and closed. The function accepts inputs such as $R_1$, $R_2$, $T_{env}$, and $T_{wax}$. It can also be manipulated to accept the cross-sectional area, chamber height, and the characteristic length and thermal conductivity of each resistor as inputs in order to easily compare model and empirical results (see section 3.2).

Figure 1.4 shows the various transient responses of the system for a range of resistances. The temperature of the chamber should rapidly increase at $t$ =0, then slowly approach the steady-state temperature. We see the hypothesis was correct: this model predicts that increasing the resistance also increases the rise time of the system. The next section will quantify that increase. From this figure, however, it appears that for the resistances we are examining, the time to reach steady sate should not be more than 200 seconds (at least, according to the model).

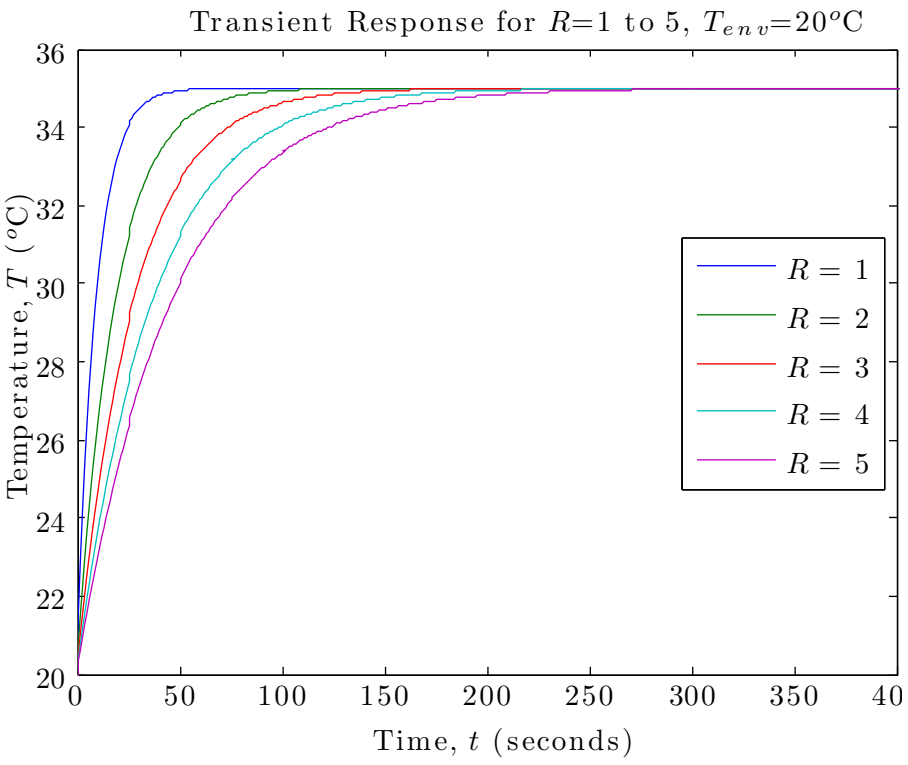


**Figure 1.4:** The graph above shows the predicted transient response of the air chamber temperature as it starts from 20°C. Here, $R = R_1 = R_2$. Wax temperature is assumed to be a constant 55°C.

**Response Time**

The time for the air temperature to complete 98% of its rise from ambient to steady-state temperature can be defined as:

$$T(t = t_{98\%}) = 0.98(T_f - T_{env}) + T_{env}. \tag{1.26}$$

Equation 1.25 at 98% of the steady-state temperature looks like:

$$T(t = t_{98\%}) = \left(T_{env} - \frac{G}{F}\right) e^{-Ft_{98\%}} + \frac{G}{F}. \tag{1.27}$$

At steady-state temperature (i.e., when $t \to \infty$), we know the exponential term disappears, so $\frac{G}{F} = T_f$. Thus, we obtain

$$T(t = t_{98\%}) = \left(T_{env} - T_f\right) e^{-Ft_{98\%}} + T_f. \tag{1.28}$$

Equating Equation 1.26 and Equation 1.28, we find

$$0.98(T_f - T_{env}) + T_{env} = \left(T_{env} - T_f\right) e^{-Ft_{98\%}} + T_f. \tag{1.29}$$

Alternatively,

$$0.02(T_{env} - T_f) = \left(T_{env} - T_f\right) e^{-Ft_{98\%}}. \tag{1.30}$$

Dividing by $(T_{env} - T_f)$ yields

$$0.02 = e^{-Ft_{98\%}}. \tag{1.31}$$

Solving for the time after which 98% of the temperature rise has occurred, we find

$$t_{98\%} = \frac{1}{F} \ln 0.02. \tag{1.32}$$

Substituting for $F$, we can obtain a more specific definition:

$$t_{98\%} = \frac{mc_p}{\frac{1}{R_1} + \frac{1}{R_2}} \ln 0.02. \tag{1.33}$$

We find, if $R_1 = R_2 = R$,

$$t_{98\%} = R\frac{mc_p}{2} \ln 0.02. \tag{1.34}$$

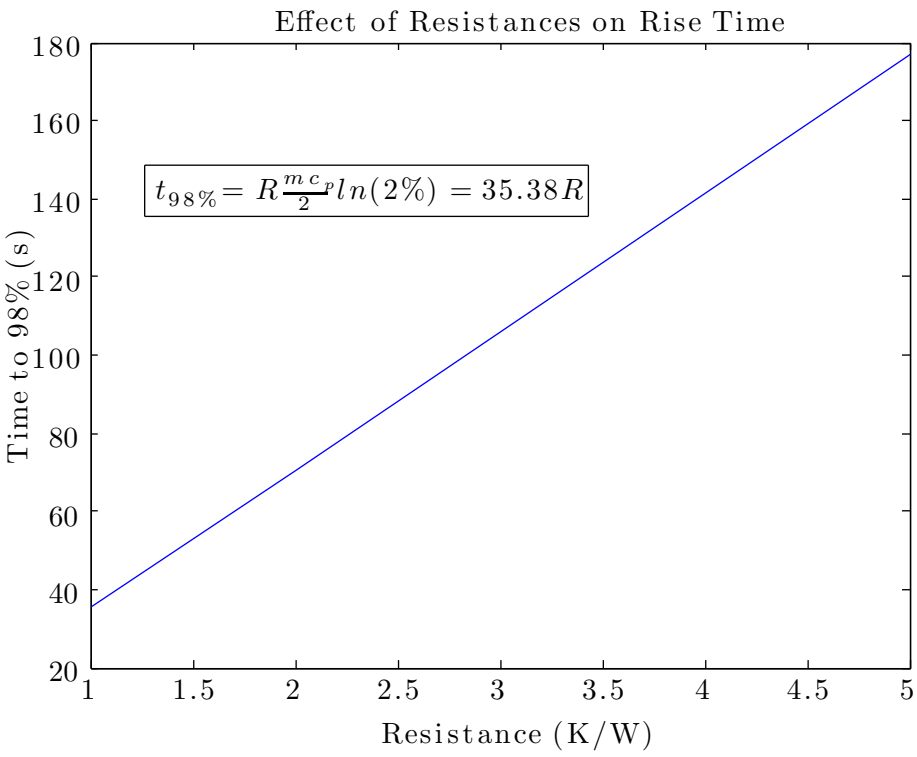


**Figure 1.5:** This graph shows the linear relationship derived in Equation 1.34.

Since $m$ and $c_p$ are scalar quantities, the 98% rise time is found to be linear with respect to resistance. Figure 1.5 illustrates the linear relationship between resistance and 98% response time demonstrated by Equation 1.34. The response time increases by 35.38 seconds per °K/W, which in comparison to total hours of usage, is not significant for the low values of $R$ being considered ($R$¡4 K/W).

The last section recommended resistances of greater than 0.75 K/W. This section has indicated that, according to the current model, most resistances will not slow down the system significantly in comparison to a two to four hour usage time. However, to minimize unnecessary increases in response time, a range of 1 to 2 K/W seems to balance mass requirements and speed requirements.

These speed predictions were challenged by experimental data, as seen in Essay 3. Additions to this model will need to be made.

## 1.2 Sensitivity to Outside Temperature

The models in section 1.1 assumed an external temperature of 20°C. In this section, environmental temperature will be varied. It is important to understand the ability of the system to operate in a range of external temperatures.

### 1.2.1 Steady-State Temperature

It is necessary to investigate how the steady-state temperature would change according to various external temperatures in which the incubator could be used. The final incubator will need to operate in various climates, and it is unlikely that the same resistances would be as effective for all external temperatures, as the temperature of the chamber would change. The relationship between the external and internal temperatures is obtained and analyzed in this section.

In the following lines, we rearrange Equation 1.8 and solve for $T_f$.

$$R_2T_f - R_2T_{wax} = R_1T_{env} - R_1T_f \tag{1.35}$$

$$(R_1 + R_2)T_f = R_1T_{env} + R_2T_{wax} \tag{1.36}$$

$$T_f = \frac{R_1T_{env} + R_2T_{wax}}{R_1 + R_2} \tag{1.37}$$

With this result, we see that if $R_1 = R_2$,

$$T_f = \frac{R(T_{env} + T_{wax})}{2R} = \frac{T_{env} + T_{wax}}{2}. \tag{1.38}$$

In other words, if $R_1 = R_2$, the internal steady-state temperature is the average of the wax's melting temperature and the external temperature.

Figure 1.6 shows the steady-state temperature of the chamber as a function of external temperature for various ratios of $R_1$ and $R_2$ ($\frac{R_2}{R_1}$), as seen in Equation 1.37. From this graph, it is clear that certain resistance ratios are more appropriate for different temperatures. The acceptable ranges are shown in Table 1.1.

**Table 1.1:** Temperature ranges for various resistance ratios (see Figure 1.6).

| $\frac{R_2}{R_1}$ | Ambient Temperature Range (°C) |
|---|---|
| 0.25 | 25 to 30 |
| 0.50 | 19 to 25 |
| 0.75 | 13 to 20 |
| 1.00 | 7 to 15 |
| 1.25 | 1 to 10 |
| 1.50 | -5 to 5 |

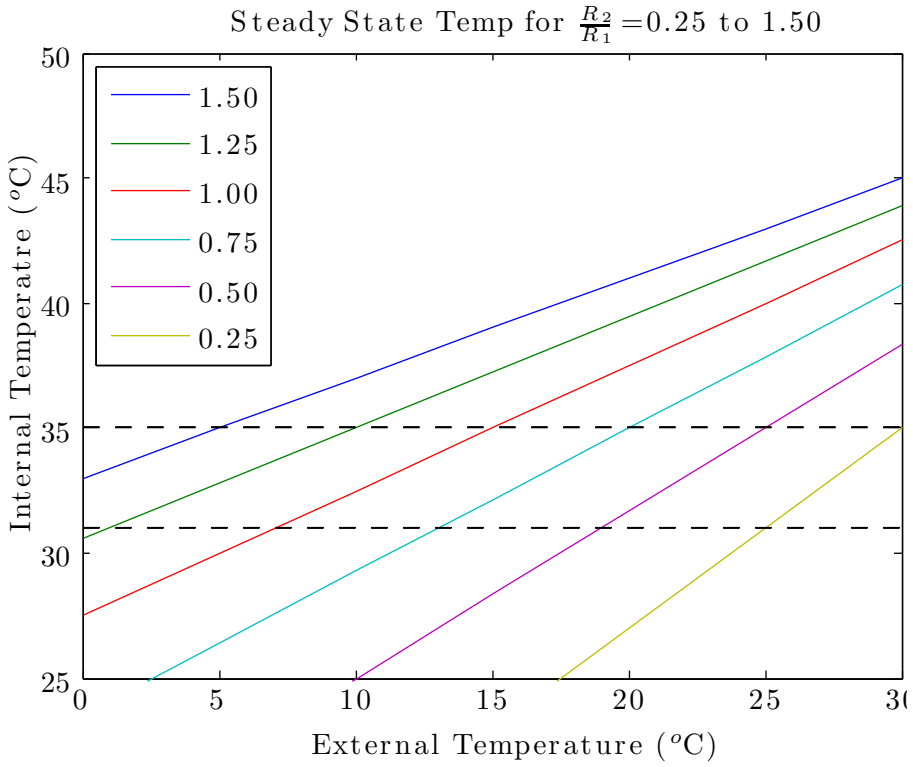


**Figure 1.6:** This graph shows the internal steady-state temperature of the chamber as a function of external temperature for various ratios of $R_1$ and $R_2$ (or, $\frac{R_2}{R_1}$). The area between the dashed lines represents the acceptable temperature range for inside the chamber (31-35°C).

Fixed ratios are not the best choice for a robust incubator. A ratio of 0.75 would work in a temperate climate, but its range still spans only seven degrees, from 13 to 20°C (for more ranges, see Table 1.1). A simple solution to this problem would be to provide various paddings and coverings for the incubator to adjust the resistance ratio as necessary for the climate or daily temperature forecast.

### 1.2.2 Required Mass

As a follow-up to subsection 1.1.2, it can be seen from Equation 1.11 that the mass required to heat the chamber depends on the steady-state temperature of the chamber, $T_f$. It can be seen from subsection 1.2.1 that $T_f$ is dependent on the environmental temperature. Combining Equation 1.11 and Equation 1.38, the mass of wax needed for two hours of heating as a function of external temperatures, assuming equal resistances, is found to be:

$$m_{wax} = \frac{T_{wax} - T_{env}}{2\Delta H^{\circ}_{fusion}} \frac{t_f}{R_1}. \tag{1.39}$$

Figure 1.7 reflects Equation 1.39's correlation between outside temperature and the mass required as well as chosen resistances. For higher resistances, the mass required is less sensitive to temperature changes, whereas for low resistances, the mass required varies greatly with changes in outside temperature. For resistances below the point where the magnitude of the slope becomes less than 1, around $0.7 \pm 0.1$ K/W, the mass requirement is more sensitive than with resistances greater than 0.7 K/W.

The maximum difference between the mass required for temperatures of 10°C and 30°C is 3.6 kg at $R$ =0.1 K/W, which decreases rapidly to 0.36 kg at $R$ =1.0 K/W, and finally to 0.036 kg at $R$ =0.01 K/W. In this model, the mass required for 30°C is will always be 50% of the mass required for 10°C. Alternatively, designing for 10°C will give the user twice as much time of use as designing for 30°C.

From this, it is recommended that the final heating element's mass be designed for operation in lower temperatures. The mass of the heating element should be selected based on a relatively low operating temperature, such as 10°C, for within the range of recommended resistances the mass penalty is minimal. If this is done, and the operating temperature is above the design temperature, there is a great benefit to the user of an increased duration of heating. Choosing the resistances to be greater than 0.7 K/W if $R_1 = R_2$ is highly recommended. This graph should also be regenerated for instances when the resistances are not equal, so the point with a dramatic change in slope can be found for different resistance ratios.

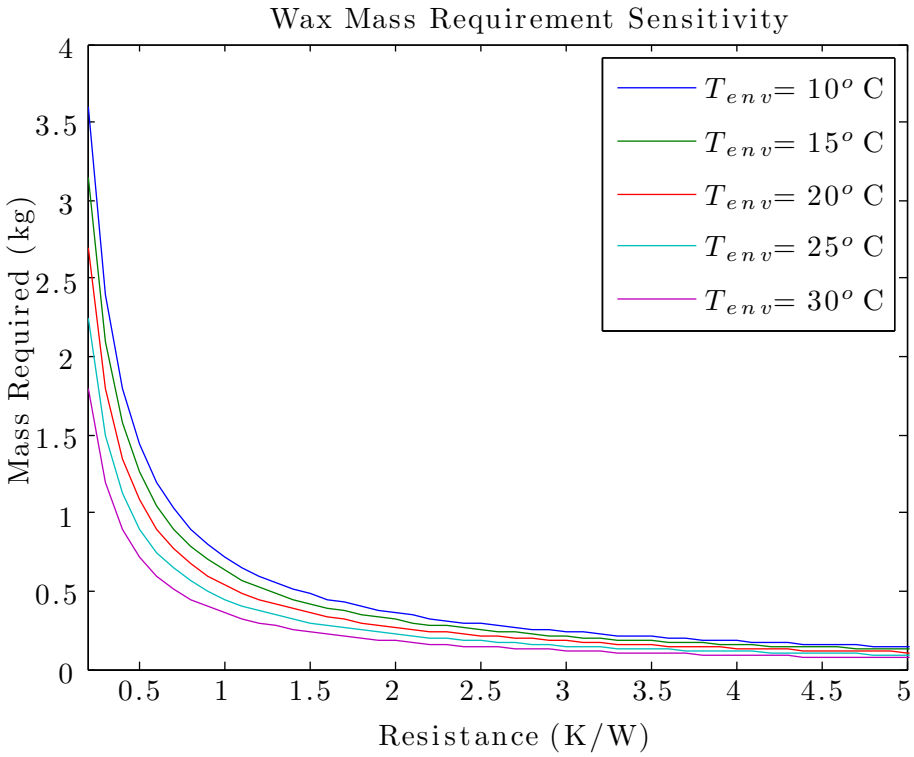


**Figure 1.7:** This figure shows the mass of wax required for two hours of heating at environmental temperatures of 10 to 30°C and resistances of 0.1 to 5 K/W.

### 1.2.3 Response Time

As seen from Equation 1.34, the 98% rise time will not change with a change in outside temperature. Because $T_{env}$ is not present in the equation, the model does not predict any difference in rise time if the environmental temperature changes. This does not seem correct, as it should take longer for the wax to heat up a cold chamber than a room temperature one. Perhaps like a time constant in a circuit, the model does not predict a difference in the time constant for different step inputs. Experimentation will be best method in determining the accuracy of these statements.

# Experimentation

## Undergraduate Thesis Essay 2

Stephanie A. Whalen

MIT Department of Mechanical Engineering

Cambridge, MA

May 17, 2012

# Experimentation


## Abstract

This essay details the experimental procedure designed to evaluate the model developed in Essay 1. Paraffin wax was melted in plastic bags submerged in boiling water. A more ideal boiling configuration for melting the wax in plastic bags was designed after trial and error, but in the future plastic bags should not be used. After melting, the wax was placed at the bottom of a portable cooler. A thin towel or blanket simulated the thermal resistance of a cotton pad or batting that will cushion the infant. Large, thin plastic container lids were used to seal the cooler instead of its typical lid, as the thin lids would more accurately simulate the material to be used for the incubator's shield. Various numbers of Vernier TMP sensors were used to measure combinations of air temperature, pad temperature, and wax temperature.

## 2.1 Overview

### 2.1.1 Wax

Wax was packaged in two separate gallon-sized plastic bags for testing. After subsequent rounds of heating, the cooled wax adhered itself aggressively to the plastic bags, and could not be removed from them (Figure 2.1). The wax and bags were placed in more plastic bags, eventually into two two-gallon plastic bags. Plastic bags are not recommended for use in this experiment, as they tend to melt very quickly if left unattended. Wax is flammable and very difficult to clean off of surfaces without damaging them, so it is recommended that a container with a higher melting temperature be used for future experimentation. However, the few kilograms of wax provided heat much longer than expected, but did take at least twenty minutes to melt in the set up used.

**Figure 2.1:** In preparation for a second round of heating, new bags had to be used. Upon removing the first plastic bag, it was found that they are weakened and prone to tearing after coming into contact with the hot pot.

### 2.1.2 Boiling

It took a few attempts to arrange the boiling set-up, although the configuration explained here is still imperfect. Polyethylene zip-top bags melt between 105 and 115°C [15]. Boiling requires a water temperature of 100°C, so the conducting surface beneath the water will be hotter. Thus, setting the plastic bags directly on the bottom of a large pot where the surface is in direct contact with the stove led to quite a bit of melted plastic and loss of some liquid wax into the boiling water. For reference, paraffin wax melts between 58 and 62°C [9]. This experiment used candle-making wax, which was found to melt over a range of 45-55°C (see subsection 3.2.2).

The addition of a straining pot, like one for spaghetti, within the first pot on the stove improved the situation, and the plastic did not melt as quickly (see Figure 2.2 and Figure 2.3).

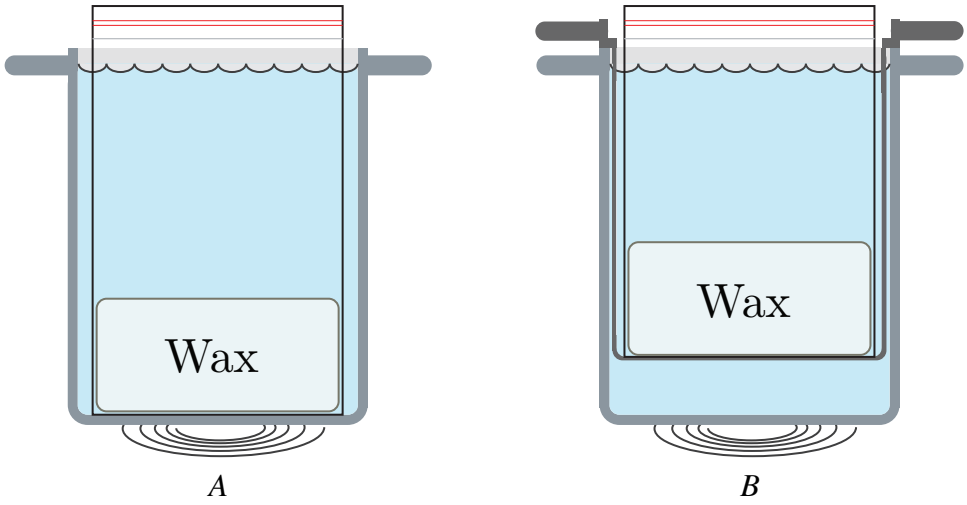


**Figure 2.2:** Boiling configuration A caused the plastic bag to melt, as the bottom of the pot was quite hot. The surface on which the plastic bag rests in configuration B was not in direct contact with the burner and therefore cooler, so it was easier to prevent the bag from melting.

### 2.1.3 Testing

Large coolers with interior dimensions similar to the proposed incubator were used for assessing the models proposed in Essay 1. To simulate the layer of padding between the baby, a thin towel or blanket was set atop the bags of melted wax (Figure 2.4).


**Figure 2.3:** Solid wax was placed into gallon-size, zip-top bags and placed into a pot with a straining pot inside. The plastic of the zip-top bags melt easily upon contact with metal surfaces directly touching the burner, so the second pot is a necessity (see Figure 2.2 for an illustration).

**Figure 2.4:** The wax, enclosed in a plastic bag for boiling purposes, was placed on top of phone books to accurately represent the height of the chamber. A towel was placed atop the wax to simulate cotton padding or other materials used to cushion the infant.

To simulate the top of the incubator, plastic container lids were used instead of the cooler lids to provide a more accurate thermal resistance between the air in the chamber and the environment (see Figure 2.5).

The cooler was assumed to be perfectly insulating, similar to the sides of the chamber in the model detailed in Essay 1. The double-walled cooler probably did not contribute significantly to heat losses, as gaps between the plastic lid and the cooler would have provided a way for the heat to escape with less resistance.

Temperature sensors (TMP variety from Vernier) in various quantities were used to detect the temperature throughout the simulation. The most important temperature to measure was the air temperature in the chamber, but other probes were added to gain further insight. The sensors were connected to the experimenter's laptop (MacBook Pro) via a Go! Link by Vernier in Test 1, and in Tests 2 and 3, via a LabPro by Vernier. Data was recorded using LoggerPro, and often the computer was left to sit with the cooler, as tests took several hours.

**Figure 2.5:** Test 1 set-up. A thin plastic lid with a 4.25" TMP probe placed through a small, drilled hole and allowed to hang in the air chamber.

## 2.2 Test 1

The first test was performed in a residential setting in a wide, open space with a constant ambient temperature of 19.8°C. In this test, only one temperature probe was used. A hole was drilled in the lid of a plastic tub, and the probe was placed through the hole that was very appropriately sized so air could not escape (see Figure 2.5).

A large, double-walled cooler was used. The air chamber's dimensions were 11"x22"x9"h, after the addition of a few phone books beneath the wax to make the chamber's dimensions more closely match that of the future incubator (see Figure 2.6).

**Figure 2.6:** Two boxes were placed in the cooler to elevate the sample and provide more insulation underneath. The two bags of wax were placed with one layer of towel above the wax.

## 2.3 Test 2

### 2.3.1 Set-Up

The second test was performed in a kitchen in a residence hall in Boston, with a less steady environmental temperature. When the experiment began, the room was 21.1°C, but the temperature likely decreased by a few degrees due to an open window. Three temperature sensors were used: one measuring the air temperature, one stuck into the wax, and one atop the blanket. A 12.5”22.5”11.5”h double-walled cooler was used. Again, a plastic lid was used, but in this instance the top probe was fed under the lid and taped to the underside of the lid, instead of dangled through a hole in the top. The sensor atop the blanket entered through the side. The probe in the wax went through a hole in the bottom of the cooler, presumably used for draining the cooler. For a photograph of the set up, see Figure 2.7.

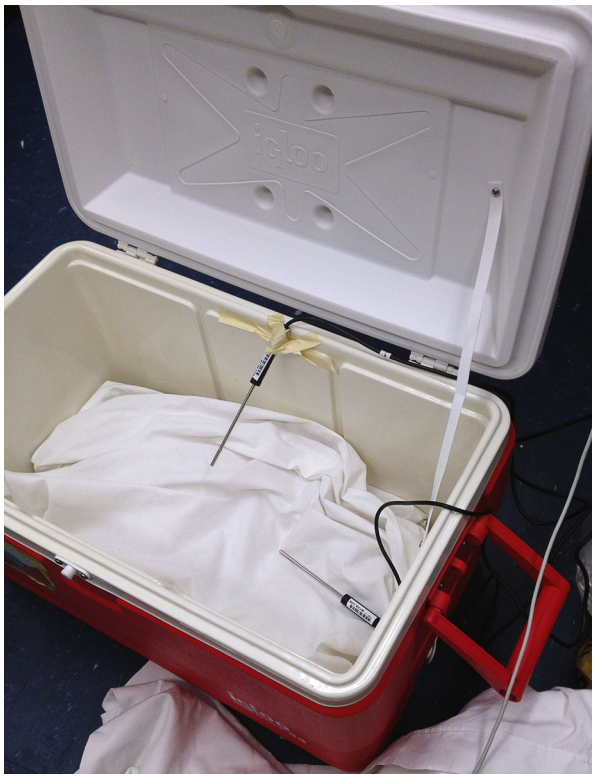


**Figure 2.7:** A photograph of the Test 2 set-up. A sensor measuring wax temperature enters through the side of the cooler (to the right in this photo).

In this test, the plastic lid did not fit perfectly on the top of this cooler, and only small amounts of tape were available. An extra blanket covered the 0.5” gap on one side of the cooler, while a weight in the form of a measuring tape normalized the upward bend of the plastic top (see Figure 2.8).

### 2.3.2 Disturbance

Unfortunately, the lid was bumped during this test. It was very clear upon returning to the test set-up that the blanket, which could now be seen on the floor, had fallen and allowed hot air to escape after 69 minutes of testing. The time of the disturbance was easily determined from a sharp corner in the temperature response (see section 3.1.2). Approximately 121 minutes into the experiment, the blanket was placed back on the test set up. This event was also visible in the data collected. Although not intentional, this event allowed us to see the incubator’s ability to recover after opening the chamber or after a leak is created.

**Figure 2.8:** Photograph of the closed Test 2 configuration.

## 2.4 Test 3

As Test 2 had some unexpected interruptions, the test was repeated. Test 3 used a similar set up to Test 2, but the cooler was placed in a space with a more stable ambient temperature. Less wax was used (due to some losses during heating), but the decrease in mass should only have affected the time that the wax would be emitting heat. The ambient temperature was 24.4°C. The room was large, but there was not a lot of air movement or devices that created heat.

# Results & Discussion

**Undergraduate Thesis Essay 3**

Stephanie A. Whalen

MIT Department of Mechanical Engineering

Cambridge, MA

May 17, 2012

# Results & Discussion


## Abstract

This essay shows, elaborates on, and discusses the results of the tests described in Essay 2. The results' steady state temperatures did not match the model, likely due to the inconsistencies between testing and modeling. For example, the model assumed a perfectly sealed chamber, while in the test environment the plastic lids chosen did not fit well. The non-steady wax temperatures also may have affected the experimental results, and caused the experiment to differ from the model, which assumes the heating element maintains a constant temperature during melting. The non-steady wax temperature is likely due to the selected paraffin being a mix of alkanes of various lengths with differing melting points. Future tests may benefit from using purer paraffins. The heating element provided heat longer than expected for all tests. The model was very inaccurate in its predictions of the transient response, particular in generating accurate rise times. The model predicted 98% rise times in seconds, while the tests showed tens of minutes instead. Efforts in reducing the experimental uncertainties would likely result in a better match between the experiment and the model, but additions need to be made to the mathematical model—most importantly, the resistance and temperature gradients of the air chamber, and the capacitance of the resistors in the thermal circuit.

## 3.1 Data Collected

### 3.1.1 Test 1

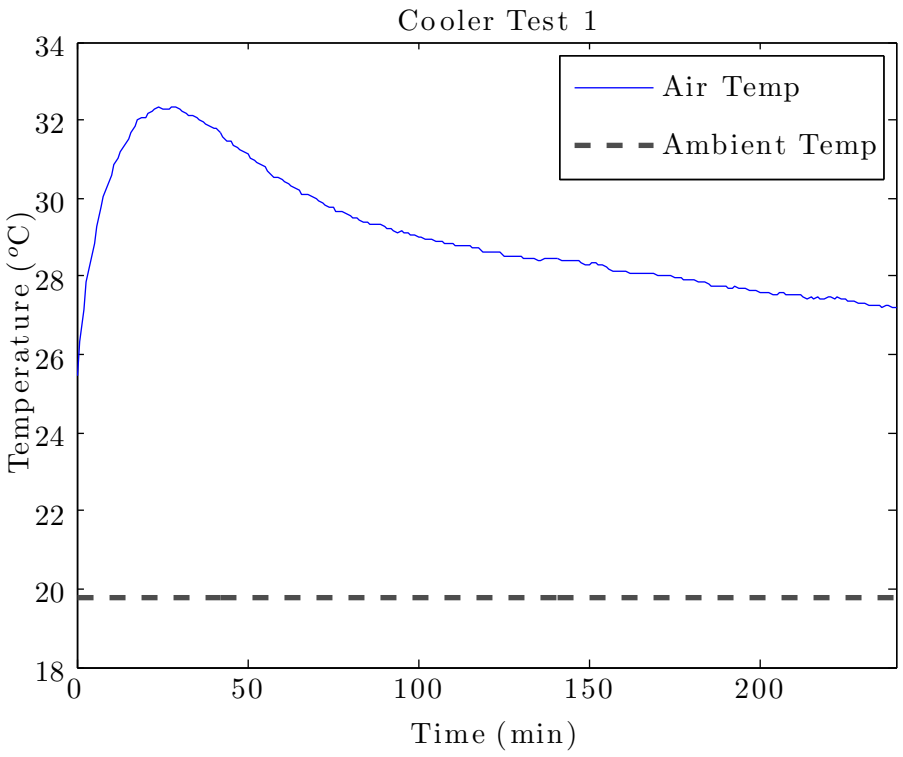


**Figure 3.1:** The collected data for Test 1. The ambient temperature was not measured in this test, but the line on the graph is the initial ambient temperature plotted for all time.

In Test 1, only the air temperature was recorded. Data collection began about ninety seconds after the lid was closed. The air temperature peaked at a temperature of 32.35°C after 29 minutes and 18 seconds (98% of rise completed in 20 minutes, 30 seconds). It then decreased at an average of -0.050°C/min for 62 minutes. The decay slowed at 91 minutes in (when $T$ =29.23°C), then declined at a slower rate of -0.014°C/min for the remaining 148 minutes. For a graphical depiction, refer to Figure 3.1. There is no clear steady-state temperature, as the temperature was never unchanging.

In a simple test of the wax solidifying in open air, a similar shape was seen (see subsection 3.2.2 for elaboration on this point).

### 3.1.2 Test 2

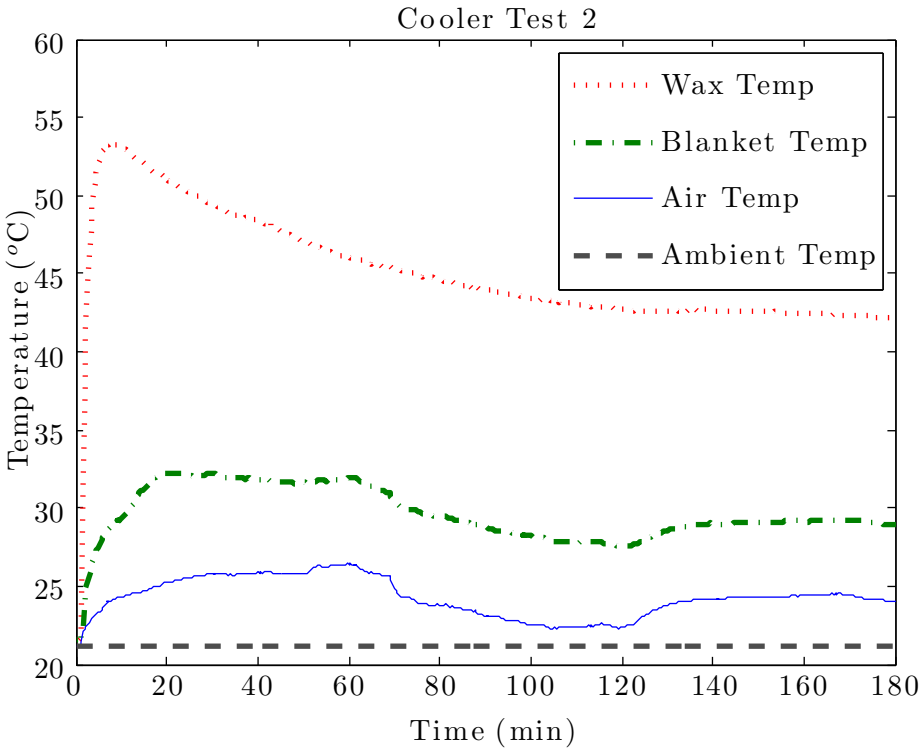


**Figure 3.2:** The collected data for Test 2. The ambient temperature was not measured in this test, but the line on the graph is the initial ambient temperature plotted for all time.

A graph of the data collected for Test 2 can be found in Figure 3.2.

#### Wax Temperature

The wax temperature peaked immediately at 53.35 °C (taking 8 minutes, 24 seconds), then decreased at an average rate of -0.093°C/min after 123 minutes and 20 seconds of testing. It remained at 42.68°C for the remainder of the test. Here, we see a similar phenomenon to the wax melting with no load (see subsection 3.2.2).

#### Blanket Temperature

The blanket temperature peaked after 19 minutes and 16 seconds at 32.33°C, and remained fairly constant. After 32 minutes of testing, the cooler was unintentionally disturbed (see subsection 2.3.2), as evidenced by the sudden decrease in blanket and air temperature shown in the data in Figure 3.2. The temperature then dropped to a local minimum of 27.56°C at 119 minutes, 20 seconds. When the lid was restored, it took 17 minutes to reach its new steady-state temperature of about 29°C.

#### Air Temperature

The air temperature reached a steady-state temperature of 25.8°C after 29 minutes and 40 seconds. A sudden elevation of temperature occurred at 50 minutes in to about 26.3°C; this pattern was also reflected subtly in the blanket temperature (see Figure 3.2). After the cooler was disturbed, the temperature rapidly decreased to 24.3°C, then declined at a slow rate of -0.06°C/min. It reached a low of 22.31°C, which is still above the initial ambient temperature of 21.1°C. Perhaps the air chamber was not able to fully reach ambient temperature due to the heat continuing to rise from the wax. The ambient temperature also may have changed slightly throughout the test, changing the overall steady-state temperature. It is surprising the opening of the chamber was not reflected in the temperature of the wax. After the cover was restored, the air temperature recovered to a new, lower steady-state temperature of 24.17°C.

### 3.1.3 Test 3

A plot of the data collected for Test 3 can be found in Figure 3.3.

#### Wax Temperature

The wax temperature peaked immediately at 54.30 °C (taking a quick 90 seconds), then decreased at a rate of about -0.138°C/min to 52.44°C at 15 minutes into the test. It then decreased more quickly at a rate of -0.187°C/min until 36 minutes and 40 seconds, when it began to decrease at a much slower rate of about -0.044°C/min for the remainder of the test.

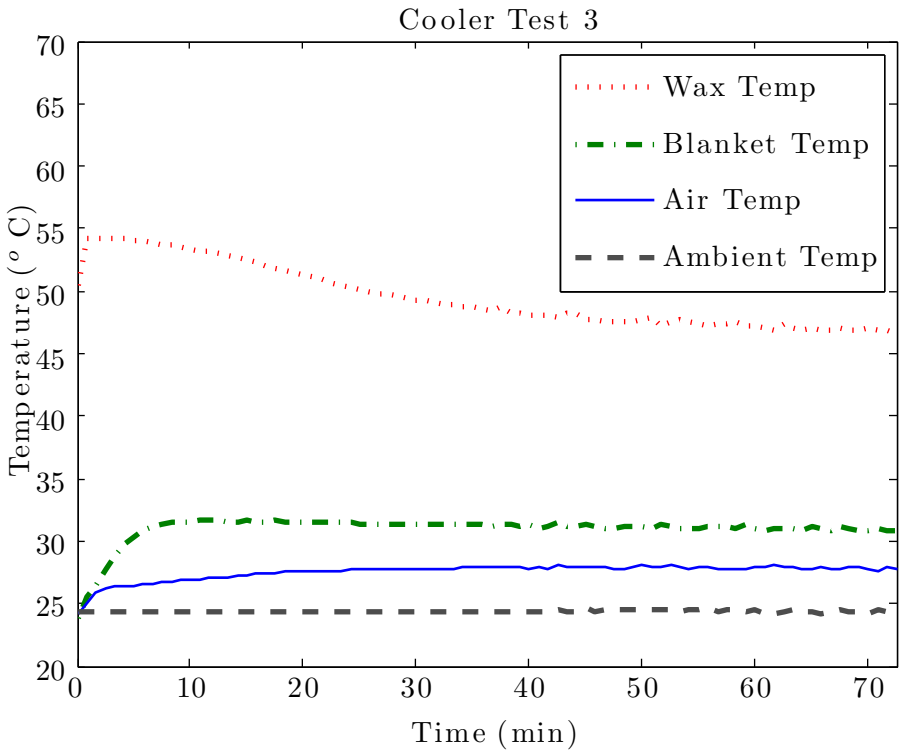


**Figure 3.3:** The collected data for Test 3. The ambient temperature was measured in this test.

It should be noted that much of the liquid wax was lost into the boiling water at one point during heating. The shorter chain alkanes would have melted first, so they likely comprised a greater percentage of the volume lost than longer-chain alkanes. The remaining paraffin would have then contained mostly longer-chain alkanes. Thus, the remaining paraffin had a higher, more uniform melting temperature. See subsection 3.2.2 for more details.

### Blanket Temperature

The blanket temperature reached a steady-state temperature of 31.65°C, in a 98% rise time of 17 minutes and 30 seconds.

### Air Temperature

The air temperature increased rapidly at the start (reaching 26.26°C in 2 minutes and 30 seconds, increasing at a rate of 0.824°C/min). After the period of rapid temperature increase passed, it increased at a much slower rate, 0.073°C/min—one-tenth of the previous rate. A steady-state temperature of 27.9°C was achieved with a 98% rise time of 32 minutes and 40 seconds.

## 3.2 Model Comparison & Discussion

Figure 3.4, Figure 3.5, and Figure 3.6 show the system's responses and the model's predictions for the properties used in the test plotted simultaneously. The following sections will discuss the trends in the model's accuracy and begin to address its shortcomings.

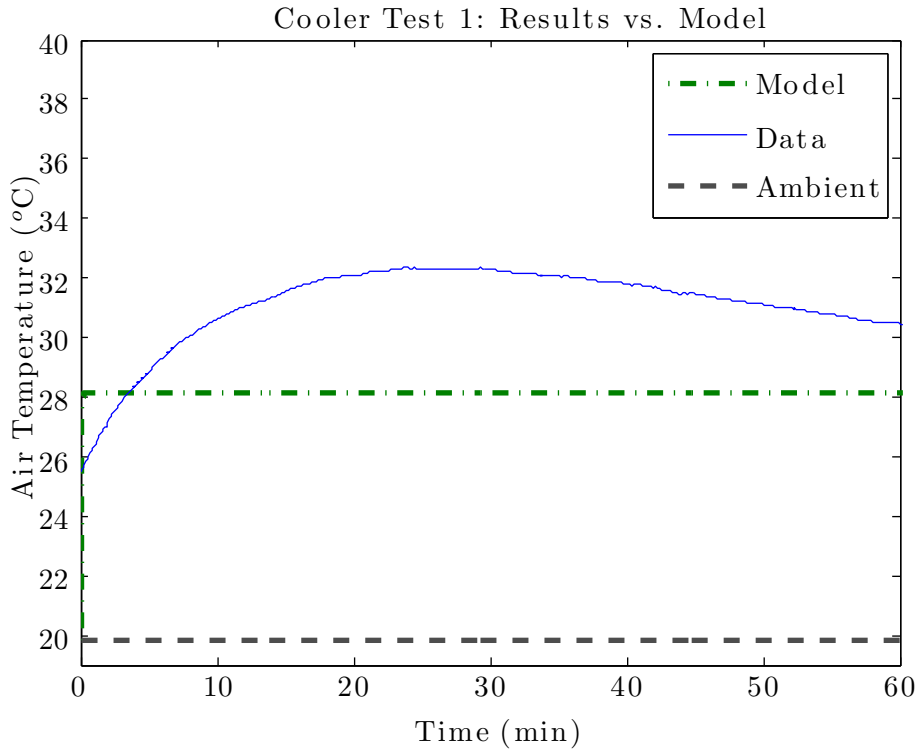


**Figure 3.4:** Comparison of the model and data for Test 1 ($R_1$ =0.2209 K/W, $R_2$ =0.0847 K/W).

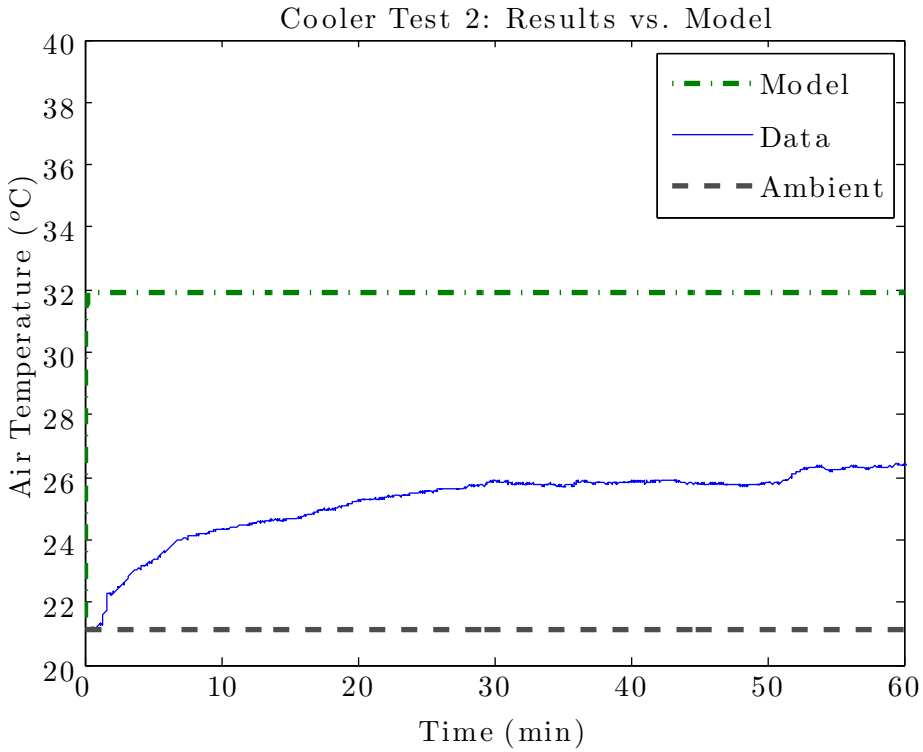


**Figure 3.5:** Comparison of the model and data for Test 2 ($R_1$ =0.1235 K/W, $R_2$ =0.0741 K/W).

**Table 3.1:** Summarizes the model and test properties. *Percent difference in steady-state temperature from 0°C; **Percent difference in steady-state temperature (as an increase from ambient).

| Test | 1 | 2 | 3 |
|---|---|---|---|
| $R_1$ | 0.2209 K/W | 0.1235 K/W | 0.1235 K/W |
| $R_2$ | 0.0847 K/W | 0.0741 K/W | 0.0741 K/W |
| $\frac{R_2}{R_1}$ | 0.3834 | 0.6 | 0.6 |
| $T_{env}$ | 19.8°C | 21.1°C | 24.2°C |
| $T_{peak}$ | 32.35°C | 26.47°C | 28.28°C |
| $T_f$ | n/a | 25.8°C | 27.9°C |
| $T_{f,model}$ | 28.17°C | 31.93°C | 34.01°C |
| $\%_1$* | n/a | -19.2% | -18.0% |
| $\%_2$** | n/a | -50.5% | -62.3% |
| $t_{98\%}$ | 22 min | 28.03 min | 32.67 min |
| $t_{98\%,model}$ | 10.2 s | 11.6 s | 11.6 s |
| % diff | 12841% | 16797% | 16798% |

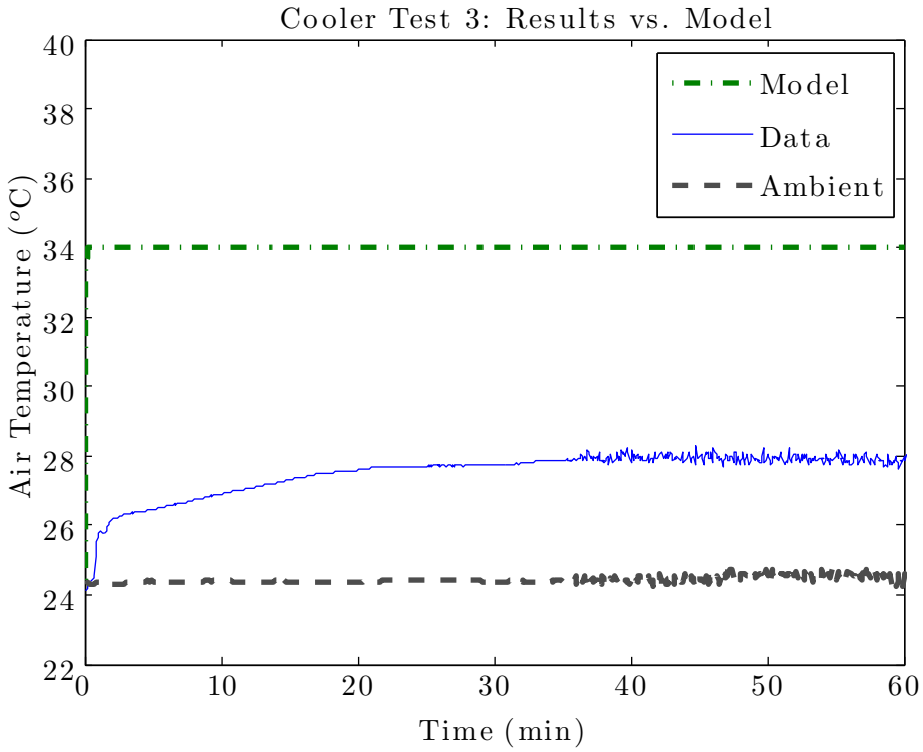


**Figure 3.6:** Comparison of the model and data for Test 3 ($R_1$ =0.1235 K/W, $R_2$ =0.0741 K/W).

### 3.2.1 Steady-State Temperature Trends

Because a steady state was not reached in Test 1, the model's steady-state value is difficult to compare. The percent error of the steady-state values as a rise from ambient temperatures for Tests 2 and 3 were -50.5% and -62.3%, respectively. The steady-state temperatures were not as high as predicted. Referring back to our model, we know that a lower-than-expected steady-state temperature indicates a lower ratio of $R_2$ to $R_1$ was present in the experiment. An imperfectly fitting lid could have produced an experimentally lower effective-$R_2$.

This is especially clear when we compare the peak temperatures between tests. Test 1 had a significantly lower environmental temperature, but reached a higher peak temperature than the other tests (see Table 3.1). In Test 1, the lid was taped securely in place; in Tests 2 and 3, the lid was less flat and it was not possible to completely seal all air gaps. This means more air was likely able to escape from the chamber, which decreased the effective thermal resistance (i.e., there was a lower $R_2$ in the test than Matlab calculated for a lid which fit properly).

### 3.2.2 Nonuniform Wax Temperatures

In a preliminary examination of the paraffin wax to determine its melting temperature, a simple test was performed: a small quantity of wax was heated by boiling water, then set out to cool at room temperature with a TMP probe inside the bag of melted wax. Two recorded temperature profiles are shown in Figure 3.7.

Normal cooling curves for a pure material would appear more like Figure 3.8: an initial drop to the melting point, a flat portion where the material is changing phase and only emitting latent heat, then another sharp drop for as it emits sensible heat and drops from the phase change temperature to ambient temperature. In Figure 3.7, the temperature profile (specifically of Test A) shows an initial sharp drop (-3.51°C/min); a subsequent, less steep drop (-0.177°C/min); followed by another sharp drop (-0.460°C/min); and lastly another less steep drop (-0.147°C/min).

The likely explanation of this phenomenon is that paraffin wax contains several different hydrocarbons of various lengths, each having unique melting temperatures (see Figure 3.9) [17]. It is likely that the first drop in Figure 3.7 is a simple decrease in sensible heat. The subsequent, flatter portion

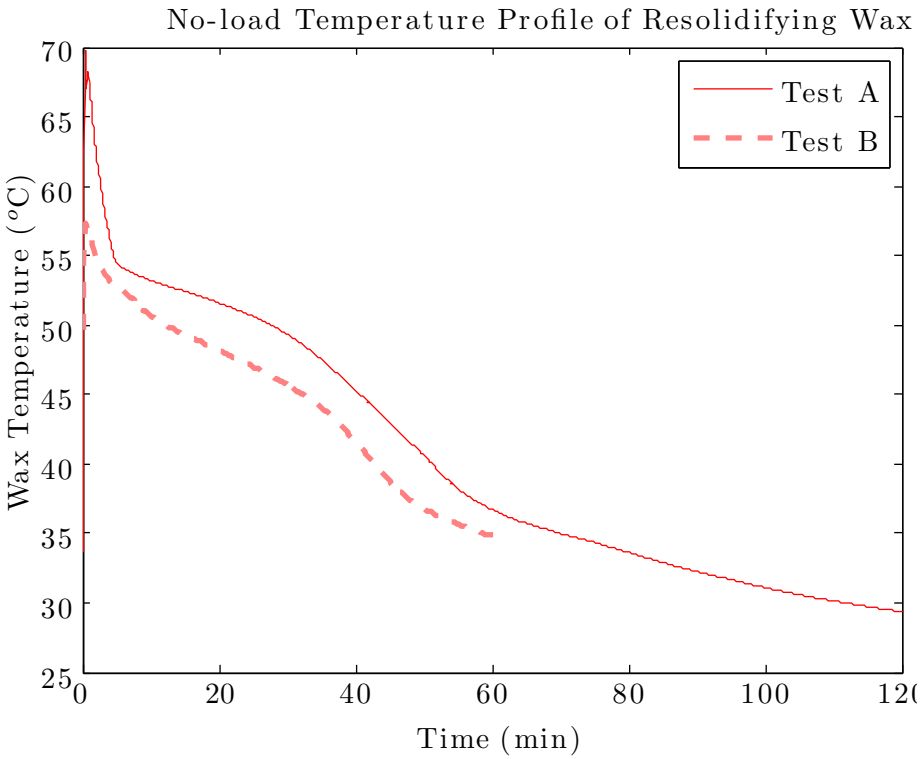


**Figure 3.7:** Graph of the no-load temperature profile of solidifying paraffin wax.

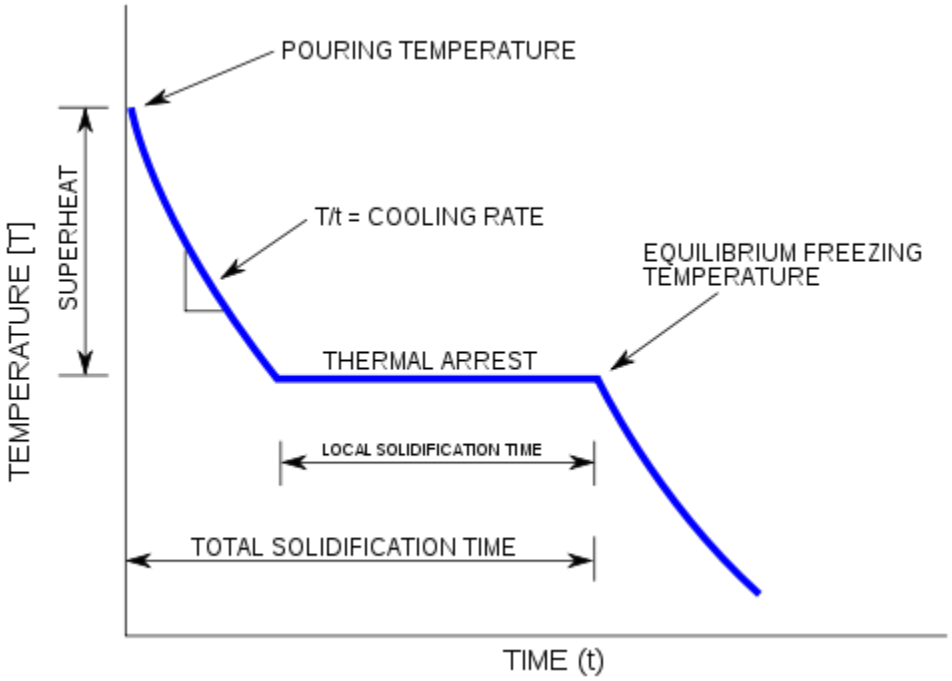


**Figure 3.8:** A typical cooling curve. Image from [16].

is a phase change of a longer alkane from a liquid to a solid which is emitting latent heat, while the other alkanes are only emitting sensible heat. The next decrease is another drop in sensible heat for more molecules. The final, gradual decay is likely occurring during the solidification of shorter alkane molecules, which are only emitting latent heat while the already-solidified and still-liquid portions emit sensible heat. The major changes in slope indicate alkane melting temperatures in two groups: one around 55°C, and the other at 38°C. Lines at these temperatures were plotted in Figure 3.9 along with various alkane melting points in order to speculate which higher alkanes may be present in the wax used in the experiments. Straight-chain alkanes (which the name 'paraffin' describes) have the form $C_nH_{2n+2}$. 'Paraffin wax' indicates a mixture of alkanes that fall within the range of $20 \leq n \leq 40$ (according to [18]) or $24 \leq n \leq 36$ (from [9]) . From Figure 3.9, it seems the paraffin wax used in the experiment (Country Lane Candle Supplies' general purpose candle making wax) contains alkanes where $n$ is between 20 and 26, likely with one group where $n$ is closer to 20 (icosane) and another where $n$ is closer to 26 (hexacosane) [17].

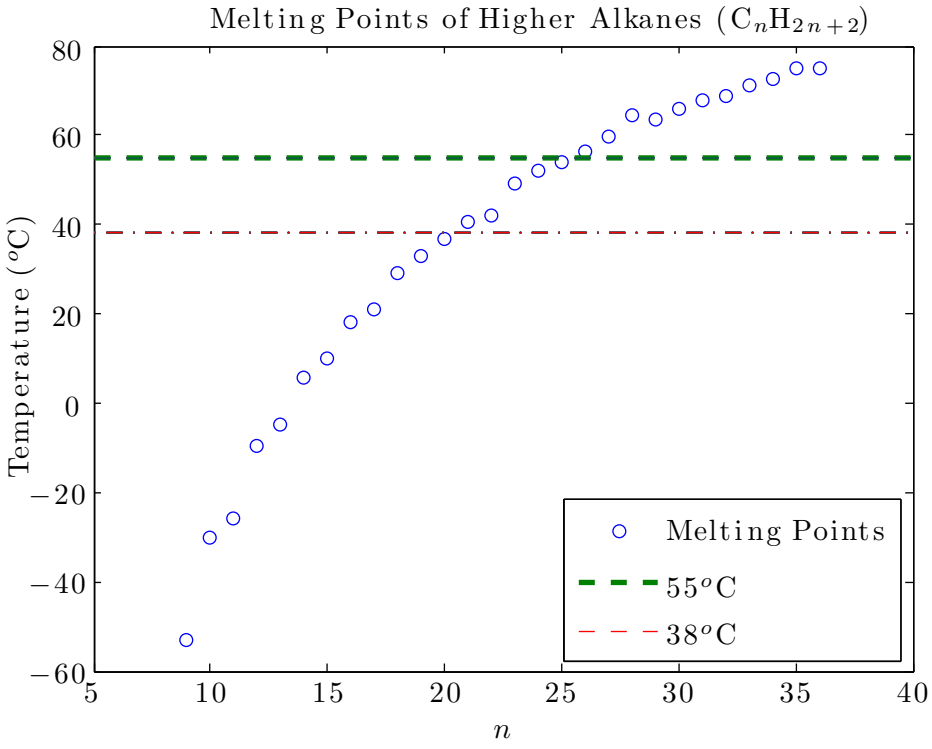


**Figure 3.9:** Graph of various alkane melting temperatures. Data from [17].

This general trend is reflected in the wax temperature profile for Test 2, and the air temperature

for Test 1. In Test 3, some liquid wax was lost in boiling. The wax that would have melted first would have been the shorter hydrocarbon chains, so the recovered wax may have been made of predominately longer chains, thus the paraffin had a more uniform melting temperature.

### 3.2.3 Length of Heating

In all tests, the wax seemed to provide heat for more than adequate amounts of time. After completion of all tests, the wax was still warm, although bits were solidified. From the transient response graphs in section 3.1, it is clear that the quantities of wax used (a few kilograms) were sufficient to provide several hours of heat. The simulations were not run for a sufficient amount of time to determine the time taken to reduce the wax to room temperature. With no load and only a small quantity of wax (Figure 3.7) sitting out at room temperature, we see it took the wax almost two hours to return to room temperature. No load implies a high heat flux out of the wax, so in a system with resistance, it would provide warmth even longer.

### 3.2.4 Transient Response

The transient response predictions of the model created in subsection 1.1.3 were very inaccurate for these experiments. The predictions for rise time were several orders of magnitude different from the experimental rise times (seconds compared to tens of minutes).

The expected reason this model fails to accurately predict the transient response is that the model does not take into account temperature gradients across the air chamber. While the Fourier Law of Conduction is suitable for this system in steady state, the gradients within the chamber and in resistor 1 must be addressed. The thermal conductivity of air is very low, which makes it a great resistor (this is why double-walled coolers are effective). Therefore, while the bottom of the chamber may quickly begin to get warm, it likely takes much longer for the air towards the top of the chamber (where $T$ was measured in this experiment) to feel the full effects of the heat the wax is providing. The thermal resistance of the air chamber should be considered in studying the transient temperature response. This property would be difficult to overcome in the future incubator

design. Every time the incubator is opened and closed, these temperature gradients would need to be overcome, and the air reheated.

The other reason this model could have failed may be due to characterizing the resistors as purely resistive devices, rather than devices with both thermal resistance and capacitance. If the blanket or towel was a pure thermal resistor, the top-side of the blanket would reach steady-state temperature (an even temperature drop) almost immediately. We see from the data taken in Tests 2 and 3 that this is simply untrue. The blanket temperatures' 98% rise times were 18 minutes, 35 seconds and 17 minutes, 30 seconds for Tests 2 and 3 respectively. The long length of time for the blanket to warm indicates a high thermal capacitance that the model simply does not account for. This could be an obstacle for the incubator design, as the baby may need the emitted heat faster than the incubator can deliver. This effect may be mitigated if the infant is lying on the surface of the resistor, however; the baby's temperature would help heat the pad so the time constant would be lower, and thus the air would heat faster.

## 3.3 Reducing Experimental Error

As detailed above, better-fitting lids would allow less heat to escape, thus experiments would be more likely to achieve the expected steady-state temperature.

The current model uses a constant temperature to model the wax melting. Using paraffins with a more uniform chemical composition would allow easier study of the air chamber temperature, because there would be less variability in melting temperature from the heat source.

## 3.4 Further Developments to the Model

As detailed in a previous section, the following adjustments would likely improve the model's ability to predict the real behavior of the incubator:

1. Accounting for a changing wax temperature, or using a pure paraffin wax so the melting temperature is more constant,

2. Accounting for the thermal capacitance of the blanket or towel (currently a simple resistor), and

3. Adding thermal resistance of the air to the circuit, and accounting for temperature gradients within the air and determining its effects on rise time.

## 3.5 Future Work

If the flaws in the experiments listed in section 3.3 are addressed, the model in Essay 1 may accurately predict steady-state temperatures. However, the transient response of this model would not accurately describe the behavior of this system to the correct time scale without the addition of the items detailed in section 3.4, or other critical considerations.

If the project's designers desire a more accurate model, the next step would be to add the resistance of the air and the capacitance of the towel to the model. A new thermal circuit must be constructed to obtain a more accurate prediction of the transient response. If the next iteration of the model predicts rise times that are in tens of minutes rather than a few seconds, then the model is progressing in the right direction.

Once the additional circuit components are added, the next model should incorporate the ambient temperature and the wax temperature as dynamic quantities in the Matlab simulation. A modified differential equation would need to be written, where $T_{env}$ and $T_{wax}$ are functions of time. Then, the measured environmental and wax temperature profiles from tests can become factors in the simulation, and the predicted air temperature profile should more closely match the measured air temperature profile.

More thorough tests should be performed, without plastic bags. A metal water bottle (as suggested by Stephen Ho) or another more effective container could be used for boiling and containment. Experiments should investigate more pure paraffin waxes, in order to see if there is a definitive advantage to using a purer material with a more uniform melting point. The range of melting points is important information in order to select proper resistances. Experiments should be performed with various paraffins to evaluate their cooling profiles.

The designers of the incubator should be consulted to discuss resistor options, including the feasible range of resistors given other aspects of the incubator design, e.g., the requirement of a transparent cover or the need for a comfortable barrier between the wax and the infant. The upper bounds of resistance for the lid and the barrier between the infant and the wax need to be identified. With the consideration of possible wax melting temperatures and resistances in mind, the steady state temperature of the air chamber in various climates can be determined. The rise time (either obtained from the adjusted model or more experimentation) should also factor into the choice of resistances.

Testing should be performed with materials that would be used in the final incubator. A better chamber should be constructed for testing, or better yet, the final incubator design should be used. If using the final design is not possible, a chamber with a better seal and of the correct size would provide for consistent testing. A more stable testing environment would ensure that the results accurately describe the incubator's behavior. More certainty in experimentation would allow designers to make the best choices possible for the final product.

## 3.6 Conclusion

The transient response of the model detailed in this thesis would not accurately describe the transient thermal response of the incubator without further modification, but it may accurately predict steady state temperatures if the flaws in the experiments are addressed. Essay 1 provides insight into the steady state temperature and mass considerations. The experimental set-up detailed in Essay 2 provides a starting point for future experimentation. The results of the experiments detailed in this essay, Essay 3, can guide the revision of the model. The progress made by this thesis in the thermal design of the incubator should advance the product into the next phases of prototyping.

# Bibliography


[1] Subhrangshu Datta and Chitro Neogy. Affordable healthcare technologies for the base of the pyramid. FrontierMed Powerpoint presentation sent to MIT members of the Anya project regarding the specifics of the incubator., January 2012.

[2] GE Healthcare. Airborne 750i Transport Incubator, 2012. URL http://www3.gehealthcare.com/en/Products/Categories/Maternal-Infant_Care/Incubators/Airborne_750i_Transport_Incubator.

[3] Whittemore Enterprises. URL http://www.wemed1.com/Products/spec.asp?ItemNumber=INC-AC300.

[4] Embrace. Product, 2012. URL embraceglobal.org.

[5] Kopernik. Embrace infant warmer. URL http://kopernik.info/technology/embrace-infant-warmer.

[6] Elaina Present. Mechanical design and prototyping of a neonatal incubator for areas with intermittent electrical grid power. Undergraduate Thesis, Massachusetts Institute of Technology, May 2012.

[7] Ben Reinhardt. Thermal energy storage, October 2010. URL http://large.stanford.edu/courses/2010/ph240/reinhardt1/. Submitted as coursework for Physics 240.

[8] Ibraham Diner and Marc A. Rosen. *Thermal Energy Storage*. Wiley, 2002.

[9] Paraffin wax. URL http://www.chemicalbook.com/ChemicalProductProperty_EN_CB2854418.htm.

[10] Ernest G. Cravalho, Jr. Joseph L. Smith, John G. Brisson, and Gareth H. McKinley. *Thermal Fluids Engineering: An Integrated Approach to Thermodynamics, Fluid Dynamics, and Heat Transfer*. MIT/Pappalardo Series in Mechanical Engineering. Oxford University Press, 2005.

[11] Originally from openclipart.org. Infant outline clip art. URL http://www.clker.com/clipart-15722.html.

[12] Matt Swann. Schematic symbols for Adobe Illustrator, August 2006. URL http://swannman.wordpress.com/2006/08/10/schematic-symbols-for-adobe-illustrator/.

[13] M.N.A. Hawlader, M.S. Uddin, and Mya Mya Khin. Microencapsulated PCM thermal-energy storage system. *Applied Energy*, 74:195–202, 2003.

[14] Charles Henry Edwards and David E. Penney. *Elementary Differential Equations with Boundary Value Problems*. Prentice Hall, 5th edition, 2004.

[15] Ldpe, 2011. URL `http://www.falatgroup.com/ProductLevel2/53/LDPE/default.aspx`.

[16] Cooling curve. URL `en.wikipedia.org/wiki/Cooling_curve`.

[17] Higher alkanes, Accessed 2012. URL `en.wikipedia.org/wiki/Higher_alkanes`.

[18] Paraffin. URL `en.wikipedia.org/wiki/Paraffin`.